RAA 2014 Vol. **14** No. **12**, 1674–1681 doi: 10.1088/1674–4527/14/12/015
http://www.raa-journal.org *http://www.iop.org/journals/raa*

Research in Astronomy and Astrophysics

Data preprocessing and preliminary results of the Moon-based Ultraviolet Telescope on the CE-3 lander

Wei-Bin Wen[1,2], Fang Wang[1,2], Chun-Lai Li[1,2], Jing Wang[1,3], Li Cao[1,3], Jian-Jun Liu[1,2], Xu Tan[1,2], Yuan Xiao[1,2], Qiang Fu[1,2], Yan Su[1,2] and Wei Zuo[1,2]

[1] National Astronomical Observatory, Chinese Academy of Sciences, Beijing 100012, China
[2] Key Laboratory of Lunar and Deep Space Exploration, National Astronomical Observatories, Chinese Academy of Sciences, Beijing 100012, China; *wangf@bao.ac.cn*
[3] Key Laboratory of Space Astronomy and Technology, National Astronomical Observatories, Chinese Academy of Sciences, Beijing 100012, China

Received 2014 July 23; accepted 2014 October 15

Abstract The Moon-based Ultraviolet Telescope (MUVT) is one of the payloads on the Chang'e-3 (CE-3) lunar lander. Because of the advantages of having no atmospheric disturbances and the slow rotation of the Moon, we can make long-term continuous observations of a series of important celestial objects in the near ultraviolet band (245∼340 nm), and perform a sky survey of selected areas, which cannot be completed on Earth. We can find characteristic changes in celestial brightness with time by analyzing image data from the MUVT, and deduce the radiation mechanism and physical properties of these celestial objects after comparing with a physical model. In order to explain the scientific purposes of MUVT, this article analyzes the preprocessing of MUVT image data and makes a preliminary evaluation of data quality. The results demonstrate that the methods used for data collection and preprocessing are effective, and the Level 2A and 2B image data satisfy the requirements of follow-up scientific researches.

Key words: Chang'e-3 mission — the Moon-based Ultraviolet Telescope — data preprocessing — near ultraviolet band

1 INTRODUCTION

The Chang'e-3 (CE-3) lunar probe was launched on 2013 December 2 from the Xichang Satellite Launch Center. It made a successful soft landing on the Moon on December 14 (Ip et al. 2014). The Moon-based Ultraviolet Telescope (MUVT) is used to observe galaxies, binary stars, active galactic nuclei and bright stars. The MUVT system is the first long-term observatory to be deployed on the Moon. A moon-based observatory has a number of advantages. The Moon's thin exosphere provides excellent opacity with no atmospheric turbulence (Wang et al. 2011). In addition, the Moon provides a stable platform. Moreover, motion of the sky as seen from the Moon is 27 times slower than on Earth, allowing extremely long, uninterrupted imaging campaigns of a target. The MUVT system is set up to perform multi-day observation activities that can monitor variable stars and active galaxies in the near ultraviolet band. Objects that are bright in the near ultraviolet band include variable stars, binaries, novae, quasars and blazers. The MUVT can continuously monitor these targets to reveal complicated optical variable behavior they might exhibit, which can effectively uncover activity in the cores of these celestial objects and the nature of physical processes that can be observed better in the near ultraviolet band than in the visible band.

From 2013 December 16 to 2014 January 22, a series of scientific explorations by the MUVT were carried out in sequence, including instrument calibrations, shafting observations that calculate the direction of the optical path in celestial coordinates, astrometric calibrations, surveys and pointing observations.

Firstly, the technical specifications, working mode and calibration of the MUVT are introduced in Section 2. Then, Sections 3 and 4 give the methods of data calibration and preprocessing for MUVT respectively. Finally, with the help of image data, the preliminary analysis for data is carried out in Seciton 4.

2 INTRODUCTION TO THE INSTRUMENT AND ON-ORBIT WORK

The MUVT covers a wavelength range of 245 to 340 nm. It is capable of detecting objects with a brightness down to magnitude 13 (Dai et al. 2014). It also has an excellent pointing system for long-term observations of targets. The image compression on the data processing system applies the lossless image compression algorithm JPEG-LS. The main specifications are shown in Table 1.

Table 1 Main Specifications of the MUVT

Index	Name	Main indicator and performance
1	Spectrum	$245 \sim 340$ nm
2	Field of view	$\geqslant 1.27^\circ \times 1.27^\circ$
3	Detection limit	1.13×10^5 counts s^{-1} m^{-2} (exposure time: 30 s, S/N: 5σ)
4	Detection sensitivity (accuracy)	0.2 mag ($5 \sim 13$ mag)
5	Effective number of pixels	$\geqslant 1024 \times 1024$
6	Spot size of energy concentration up to 80%	$\leqslant 3 \times 3$ pixels
7	Telescope aperture	15 cm
8	Quantization value (digital bit number)	$\geqslant 8$

In terms of functionality of the modules, the MUVT system consists of a telescope, detector, reflector, swivel table, control system and accessory equipments. The MUVT system uses a pointing mirror that features a two-dimensional gimbal to track objects. It can collect radiation from the sky and image on the focal plane through the optical filter. The MUVT instrument consists of a Ritchey-Chretien telescope (RCT) that is a specialized Cassegrain telescope using a hyperbolic primary mirror and a hyperbolic secondary mirror to eliminate third-order coma and spherical aberration. RCT designs are well-suited for wide-field and photographic observations that have good off-axis performance with a large field of view free of optical errors. Figure 1 shows the main body and mounting platform of the MUVT. Figure 2 is the optical path of the MUVT system (Jia et al. 2014).

The CE-3 probe landed in Mare Imbrium, 44° north of the lunar equator. The MUVT is mounted in cabin-Y of the lander. Therefore, the best option for scientific observations is in a direction near the north celestial pole. During two lunar daytime periods from 2013 December 16 to 23 and from 2014 January 12 to 23, the observation mission performed by the MUVT included astrometric calibration, photometric calibration and surveys. In total, it has worked for about 170 hours collecting all kinds of images, including 166 uncompressed full-sized images with dimension of 1024×1024, 14 412 compressed full-sized images and 66 pieces of uncompressed window images. During the working time of the lunar day, the MUVT operated well, with engineering and telemetry parameters staying in an appropriate range.

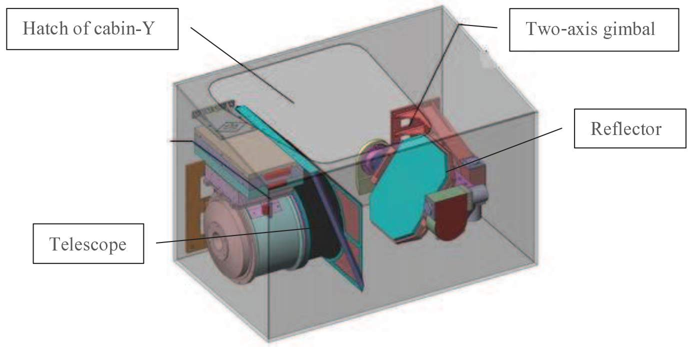

Fig. 1 Telescope body and mounting platform that uses a two-axis gimbal.

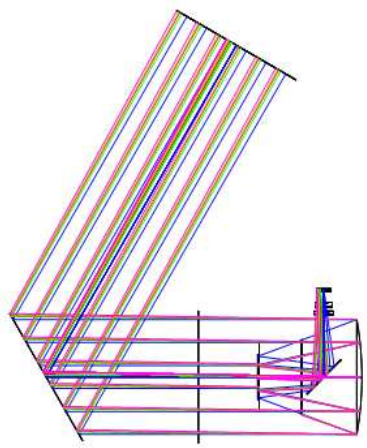

Fig. 2 The optical path of the MUVT system.

3 CALIBRATION

The calibration of MUVT can be divided into two parts, the ground calibration and on-orbit calibration. Ground calibration and related tests mainly include instrument correction and system response measurement. The flat field calibration for a CCD can be used to monitor the uniformity in the response of a CCD used for ultraviolet observations; on the other hand, it can also be used to correct nonuniformity between pixels. The flat field for the system can be used to correct nonuniformity in the system response. Because of nonuniformity in the LED's flat field on the MUVT, the LED's flat field data are used for monitoring the change in heterogeneity of individual pixels in orbit, carrying out calibration for the CCD. According to the requirements for calibration, the bias, dark and flat field calibration matrixes are obtained for different environmental conditions and different parameter sets. It is found that the dark current intensity shows a relationship with the exposure time and the working temperature of the CCD chip. By applying overscan correction and bias field correction, dark current data are divided into groups on the basis of the temperature and exposure time, and then are combined and averaged, eliminating the effects of cosmic rays. The dark current calibration matrix is obtained. By analyzing the results, it can be found that monochrome flat field data have no obvious changes, and nonuniformity in the response of the CCD to photons remains stable. By division between LED flat field data and white flat field data, the results show that nonuniformity in the response still exists among pixels, and the degree of nonuniformity in the response strongly depends on the type of spectrum, so the LED flat field data cannot be used for instrument correction. With quantitative flat field analysis of the system, the uniformity in illumination is good. The flat field data for the system can be used as a calibration matrix for nonuniformity correction of response during exploration. By overscan correction and dark field correction, the flat field data are divided into groups according to the temperature and the exposure time, and are then combined and averaged. A normalized flat field calibration matrix is obtained. In the ultraviolet CCD calibration experiment, the data on the quantum efficiency of the CCD maintain a good consistency between images, with less than a 5% deviation, compared with what is determined from the manufacturer. On orbit, the calibration items include instrument correction, attitude calibration and photometric calibration. The instrument correction on orbit includes bias field correction, dark current correction and flat field correction. Close to the beginning and end of each lunar day, after the MUVT powers on and the hatch closes, a group of images that are used for instrument correction must be taken; due to the uneven illumination, the flat field data can only be used to correct the nonuniformity in the response between pixels, being used in combination with the flat field data taken on the ground. This paper will give preliminary results after ground calibration and in-flight calibration processing are combined with MUVT preprocessing.

4 DATA PREPROCESSING AND PRELIMINARY RESULTS

Figure 3 shows a flowchart describing the data preprocessing method used for MUVT (Tan et al. 2014). The flowchart mainly includes the following steps. First, data communication channel processing includes: frame synchronization, Reed-Solomon decoding and optimized selection of two possible ground stations; Second, the frame data are compartmentalized and sent to appropriate subsequent processing routines according to the identifier of the payload, generating Level 0A data products, the source packet data from MUVT; cutting off the frame header, splicing the scientific segmentation from the MUVT source packet data, which generate the Level 0B data products; in order to label data from different Earth days into data blocks, after physical conversion is performed, these generate Level 1 data products; Level 2A data processing is related to instrument correction; Level 2B data produce the results for processing related to identifying location.

The following is mainly concerned with how the preprocessing method is related to Level 2A and Level 2B data products and preliminary results.

4.1 Instrument Correction

Each frame taken by the MUVT system consists of two parts: a frame header and scientific segmentation. The scientific segmentation can be subdivided into the overscan, dark and pixel parts, which are illustrated in Figure 4.

The overscan correction is at first performed on all the images taken by MUVT. For each of the frames, the corresponding overscan level in each CCD row is determined by a polynomial fitting after a binning of the overscan records in both the row and column directions on the CCD. Because the MUVT system works in the lunar day, sunshine is the main source of stray light. To remove contamination due to stray light, we at first group images in each observational run by their pointings. In addition, the total time that elapsed in each group is required to be no more than 30 min to avoid a significant change in the level and pattern of stray light with time. In each group, the pattern of stray light in a given image is constructed by combining all the images (except the given image) in the group without any shift. Contamination from stray light is subsequently removed from a given image by subtracting the constructed pattern of stray light whose level is determined by the ground level of the given image. It is noted that this procedure not only removes the pattern of stray light,

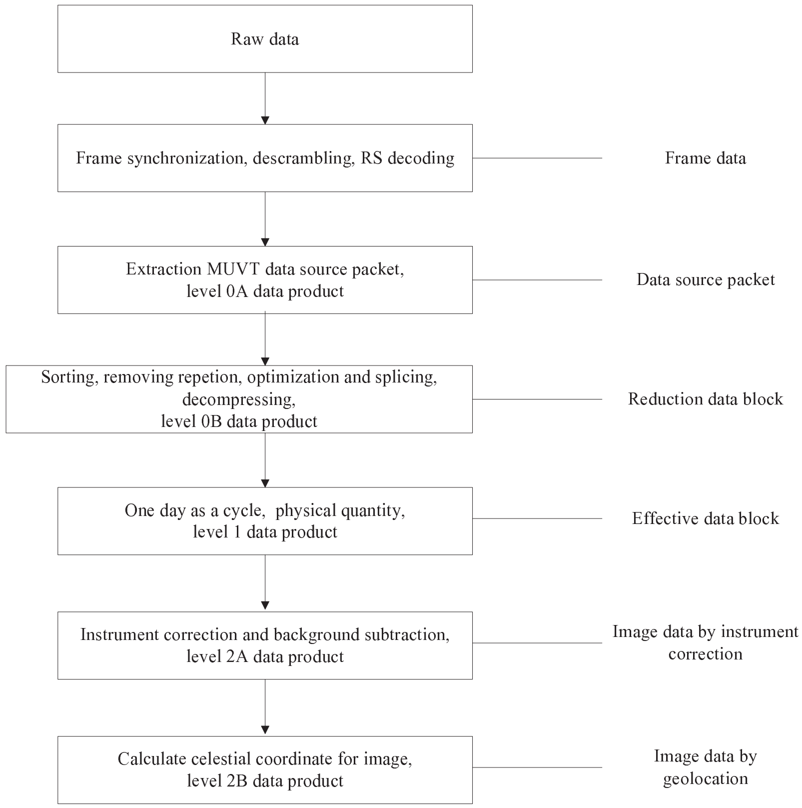

Fig. 3 Data preprocessing of the MUVT system.

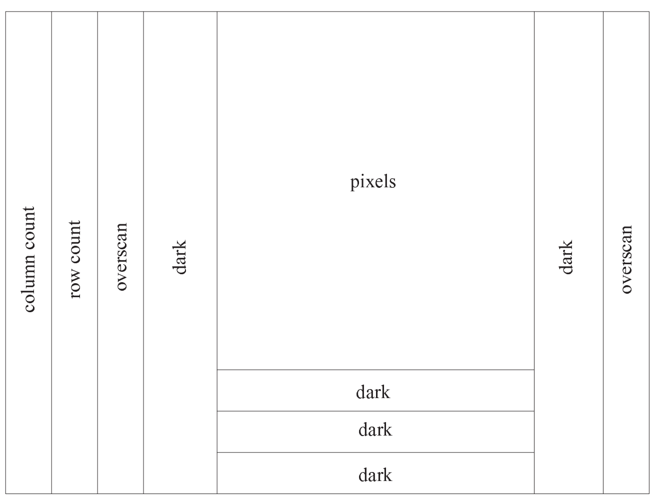

Fig. 4 The data format of the MUVT system.

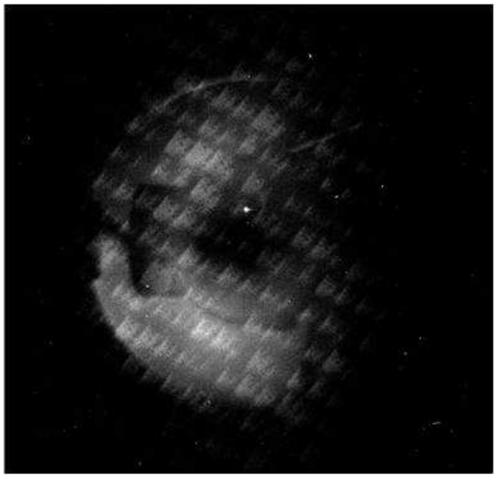

Fig. 5 Raw image of the object.

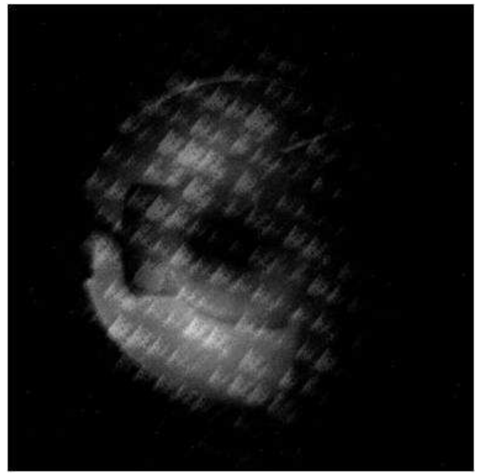

Fig. 6 Image of stray light.

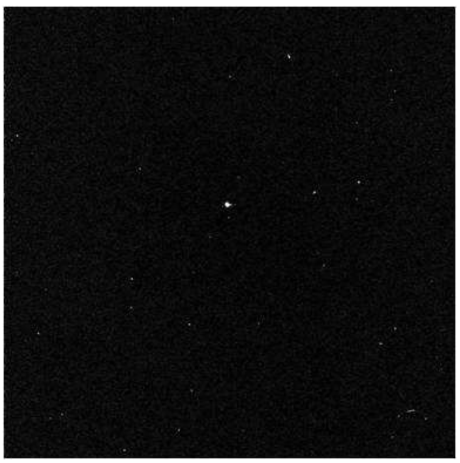

Fig. 7 Image of the object minus the stray light.

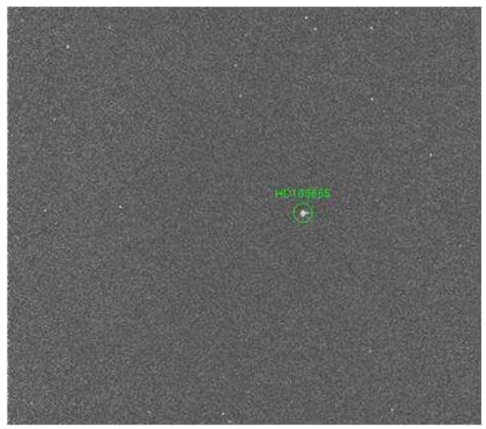

Fig. 8 Image after processing was applied which shows the target star HD 188665.

but also both underlying bias and dark current simultaneously. Flat field correction is then finally performed for all the images after stray light has been removed. The removal of stray light is shown in Figures 5 to 7 as an illustration, based on an image taken on 2014 January 22.

4.2 Point Spread Function

Regarding the concentration of starlight that falls on the detector, the target star, HD 188665 with a high signal to noise ratio (SNR), was selected. The data were acquired on 2013 December 23. A typical point spread function produced by the MUVT is shown in Figures 8 and 9 for the standard star HD 188665. Fitting the light distribution by a 1-dimensional Gaussian returns an FWHM for the pixels, which indicates that more than 80% of the energy is enclosed within 3×3 pixels for a point source (Yang & Wu 2012).

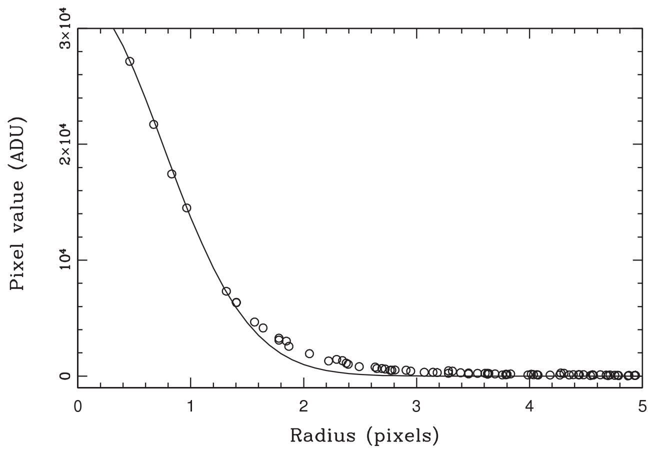

Fig. 9 ADU value distribution curve resulting from aperture photometry.

4.3 Astrometry

The celestial coordinates in the J2000 mean equatorial coordinate system are calculated for the center and the four corners for each of the images (Cao et al. 2011). The calculation is based on the pitch and azimuth angles of the gimbal and on the relationship between the attitude of the telescope and the pole that describes lunar rotation. The relationship was determined by a survey of the sky immediately after the first light of MUVT. We compare the calculated celestial coordinates and those determined by a cross-matching between the identified stars and a known catalog by using the images taken from 2014 February 13 to 15. There are 37 different pointings in total. The maximum deviation between the coordinates obtained through the different methods is about 0.2°.

4.4 Photometry System and Magnitude Zero Point

The AB magnitude system is adopted by MUVT (Yan et al. 2000). The magnitude is defined by the following equation

$$\mathrm{mag}_{\mathrm{AB}} = -2.5\lg\frac{\int f_v \cdot S_v \cdot d\ln v}{\int S_v \cdot d\ln v} - 48.6\,, \tag{1}$$

where f_v is the specific flux of a given object in units of $\mathrm{erg\ s^{-1}\ cm^{-2}\ Hz^{-1}}$ and S_v is the system's response at frequency v, including the contributions from the telescope, filter and CCD. The system's response has been determined in a laboratory. The apparent brightness m_{app} of an object could be converted from its instrumental magnitude m_{inst} according to Equation (2).

$$m_{\mathrm{app}} = m_{\mathrm{inst}} + Z\,, \tag{2}$$

where Z is the zero point for magnitude that should be determined through observations of standard stars.

Based upon observations of the standard star HD 188665 (spectral type B5V) at the beginning the MUVT mission and the data reduction described above, we obtained preliminary results on the zero point for magnitude of $Z = 17.49 \pm 0.02$ mag, in which the error corresponds to a 1σ significance level and is obtained from multiple observations.

Figure 10 shows the results when the target star is repeatedly observed with the same aperture and parameters settings. The 1σ dispersion in aperture photometry is 0.06 magnitude.

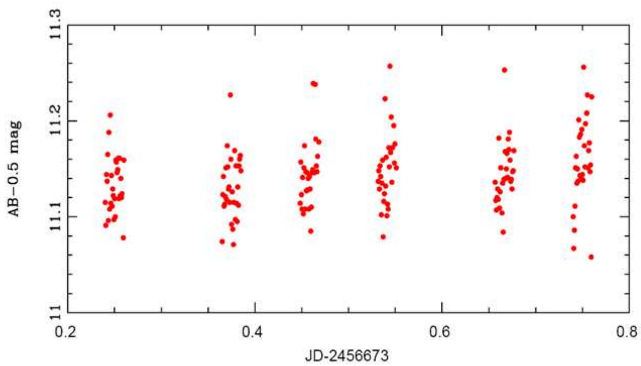

Fig. 10 The dispersion analysis for the target obtained by multiple samplings.

5 CONCLUSIONS

The MUVT is one of the payloads equipped on the lander. This is the first time the continuous monitoring of important optical variables and surveys of an area with low galactic latitude have been performed. It has worked at least one year in accordance with the design life of the instrument on the Moon. The MUVT operates in three modes: standby mode, the state of being powered on but not collecting data; adjusting mode, the state where adjustments and pointings are made; detection mode, saving data received while the device is operating. Through the analysis of data products from the first and second lunar days, instrument correction and stray light reduction are performed for all images, so the effects of the instrument and stray light are effectively removed. According to the results of data analysis, the instrument could observe magnitude 13 stars (with an SNR of 5) in a 30 s exposure during the Moon's twilight period. However, at about lunar noon, due to the interference of stray light from the Sun, the observation capacity is reduced to about magnitude 11 (with an SNR of 5). The preprocessing method is reasonable and the data products are effective. All data products can be used in a database about scientific research on ultraviolet astronomical observations.

Acknowledgements We wish to thank all members from the Ground Research and Application System (GRAS) and the Moon-based Ultraviolet Telescope instrument group (Key Laboratory of Space Astronomy and Technology) that is part of the Chang'e-3 program, whose joint efforts have made the data acquisition and preprocessing used for this study possible.

References

Cao, L., Ruan, P., Cai, H., et al. 2011, Science China Physics, Mechanics and Astronomy, 54, 558
Dai, S. W., Jia, Y. Z., Zhang, B. M., et al. 2014, Science China: Technological Sciences, 44, 361
Ip, W.-H., Yan, J., Li, C.-L., & Ouyang, Z.-Y., 2014, RAA (Research in Astronomy and Astrophysics), 14, 1511
Jia, Y., Dai, S., Wu, J., et al. 2014, Chinese Journal of Space Science, 34, 219
Tan, X., Liu, J., Li, C., et al. 2014, RAA (Research in Astronomy and Astrophysics), 14, 1682
Wang, J., Deng, J. S., Cui, J., et al. 2011, Advances in Space Research, 48, 1927
Yan, H., Burstein, D., Fan, X., et al. 2000, PASP, 112, 691
Yang, G. P., & Wu, W. T. 2012, Progress in Astronomy, 30, 467